



A new TROPOMI product for tropospheric NO₂ columns over East Asia with explicit aerosol corrections

Mengyao Liu¹, Jintai Lin¹, Hao Kong¹, K. Folkert Boersma^{2,3}, Henk Eskes², Yugo Kanaya⁴, Qin He⁵, Xin Tian^{6,7}, Kai Qin⁵, Pinhua Xie^{6,7,8}, Robert Spurr⁹, Ruijing Ni¹,
5 Yingying Yan¹⁰, Hongjian Weng¹, Jingxu Wang¹

¹Laboratory for Climate and Ocean-Atmosphere Studies, Department of Atmospheric and Oceanic Sciences, School of Physics, Peking University, Beijing, China

²Royal Netherlands Meteorological Institute, De Bilt, the Netherlands

³Meteorology and Air Quality department, Wageningen University, Wageningen, the
10 Netherlands

⁴Research Institute for Global Change, Japan Agency for Marine-Earth Science and Technology (JAMSTEC), Yokohama 2360001, Japan

⁵School of Environment and Geoinformatics, China University of Mining and Technology, China University of Mining and Technology, Xuzhou, Jiangsu, 221116,
15 China

⁶Institutes of Physical Science and Information Technology, Anhui University, Hefei, 230601, China

⁷Key laboratory of Environmental Optical and Technology, Anhui Institute of Optics and Fine Mechanics, Chinese Academy of Science, Hefei, 230031, China

⁸CAS Center for Excellence in Urban Atmospheric Environment, Institute of Urban Environment, Chinese Academy of Sciences, Xiamen 361021, China
20

⁹RT Solutions Inc., Cambridge, Massachusetts 02138, USA

¹⁰Department of Atmospheric Sciences, School of Environmental Studies, China University of Geosciences (Wuhan), Wuhan, China

25 *Correspondence to:* Jintai Lin (linjt@pku.edu.cn)

Abstract

We present a new product with explicit aerosol corrections, POMINO-TROPOMI, for tropospheric nitrogen dioxide (NO₂) vertical column densities (VCDs) over East Asia, based on the newly launched TROPospheric Monitoring Instrument with an
30 unprecedented high horizontal resolution. Compared to the official TM5-MP-DOMINO (OFFLINE) product, POMINO-TROPOMI shows stronger concentration gradients near emission source locations and better agrees with MAX-DOAS measurements ($R^2 = 0.75$, NMB = 0.8% versus $R^2 = 0.68$, NMB = -41.9%). Sensitivity tests suggest that implicit aerosol corrections, as in



TM5-MP-DOMINO, lead to underestimations of NO₂ columns by about 25% over the polluted Northern East China region. Reducing the horizontal resolution of a priori NO₂ profiles would underestimate the retrieved NO₂ columns over isolated city clusters in western China by 35% but with overestimates by more than 50% over many offshore coastal areas. The effect of a priori NO₂ profiles is more important under calm conditions.

1. Introduction

Nitrogen oxides (NO_x = NO + NO₂) are crucial gaseous pollutants in the troposphere. NO_x lead to the production of particulate matter and ozone (O₃) and enhance levels of oxidants in the troposphere (Shindell et al., 2009), which affect air quality (Dentener et al., 2003) and human health (Hoek et al., 2013). Satellite remote sensing is widely used to monitor levels of nitrogen dioxide (NO₂) pollution worldwide (McLinden et al., 2014; Krotkov et al., 2016; Ott et al., 2010; Russell et al., 2011; Lin et al., 2010). The TROPOspheric Monitoring Instrument (TROPOMI), which was jointly developed by the Netherlands and Europe Space Agency (ESA) (Veefkind et al., 2012) and was launched on October 13th 2017, is a UV/Visible/Near-Infrared/Short-wave infrared backscattering sensor onboard the sun-synchronous Sentinel-5 Precursor (S5P) satellite with an overpass time of 13:30 local solar time. With a wide swath of 2,600 km and an unprecedentedly high horizontal resolution of 3.5 × 7 km², (3.5 × 5.5 km² since 6 August 2019) TROPOMI achieves daily global coverage. This high horizontal resolution and good spatial coverage, combined with the very high signal-to-noise ratio, enables the instrument to resolve NO₂ pollution from point sources, medium-size urban centers, highways or rivers, tasks that were difficult to achieve before.

Retrievals of tropospheric NO₂ vertical column densities (VCDs) in the UV/Vis spectral range from satellite instruments consist of three steps: (1) using the Differential Optical Absorption Spectroscopy (DOAS) to fit the slant column density (SCD) of NO₂ along the light path, (2) subtracting the stratospheric contribution from the SCD to obtain the tropospheric SCD, and (3) converting the tropospheric SCD to the tropospheric VCD by using the calculated air mass factor (AMF). For TROPOMI, the random uncertainty of the total SCDs is ~ 0.6 × 10¹⁵ molec·cm⁻² considerably smaller than for the Ozone Monitoring Instrument (OMI, ~ 0.8 × 10¹⁵ molec·cm⁻², (Zara et al., 2018)). The (total or stratospheric) bias is generally between 0 and -10% according to SAOZ observations (Eskes et al., 2019), which meets the error requirements as defined in the S5P Calibration and Validation Plan (Goryl et al., 2017). The calculation of the AMF introduces the dominant source of error in the retrieved tropospheric NO₂ VCDs over polluted areas (Boersma et al., 2011; Lorente et al., 2017; Boersma et al., 2018; Lin et al., 2014; Boersma et al., 2004). The median negative biases of the daily comparisons between tropospheric VCDs from the Dutch



official TM5-MP-DOMINO (OFFLINE) product and MAX-DOAS measurements are generally less than 50% (the allowable bias is 25-50% (Goryl et al., 2017)) but quite variable with the stations and NO₂ levels, especially at polluted locations (Eskes et al., 2018; van Geffen et al., 2019).

5 TM5-MP-DOMINO uses implicit aerosol corrections by assuming aerosols to be “effective clouds”, as assumed in most satellite NO₂ products except POMINO (Liu et al., 2019; Lin et al., 2014; Lin et al., 2015). In addition, TM5-MP-DOMINO employs a priori NO₂ profiles from the TM5 model at a relatively coarse horizontal resolution (1° × 1°) (Williams et al., 2017). The implicit aerosol corrections (Lin et al., 2014; Lorente et al., 2017; Liu et al., 2019) and the coarse horizontal resolution of a priori NO₂ profile data (Laughner et al., 2016; Russell et al., 2011; McLinden et al., 2014) may be the largest sources of the large biases observed between TM5-MP-DOMINO and MAX-DOAS. Based on previous studies for OMI, implicit aerosol corrections can lead to more than 50% uncertainties over polluted areas with high aerosol loadings like China (Lin et al., 2014; Lorente et al., 2017; Liu et al., 2019). Eskes et al. (2018) showed that using a priori NO₂ profiles from the regional CAMS model at a 12 × 12 km² resolution to replace the TM5 NO₂ profiles increase the retrieved NO₂ VCDs by ~0 to 50% over Western Europe depending on the location.

Here we present a new TROPOMI tropospheric NO₂ VCD product over East Asia, namely POMINO-TROPOMI. This product is based on our POMINO algorithm (Liu et al., 2019; Lin et al., 2014; Lin et al., 2015) previously applied to OMI. POMINO-TROPOMI improves upon TM5-MP-DOMINO by employing explicit aerosol corrections and using high-resolution (~25 km) a priori NO₂ profiles, among other improvements. POMINO-TROPOMI NO₂ VCD data over July-October 2018 are presented and validated by MAX-DOAS measurements, along with additional sensitivity tests of the effects of aerosol representations and a priori NO₂ profiles.

2. Method and Data

2.1 POMINO-TROPOMI retrieval algorithm and product

As one of the UV/Vis backscatter instruments to observe NO₂, TROPOMI inherits much of the design of OMI (Veefkind et al., 2012). Thus the POMINO-TROPOMI algorithm here largely follows our previous POMINO algorithm (Liu et al., 2019), with some modifications to adapt to its high horizontal resolution and different cloud retrieval procedure.

The POMINO-TROPOMI algorithm focuses on improving the calculation of tropospheric AMF. It thus takes the tropospheric SCD data from TM5-MP-DOMINO (OFFLINE), which are obtained by fitting the 405-465 nm wavelength range with the



DOAS method. Our tropospheric AMF calculation is done for 437.5 nm, following TM5-MP-DOMINO.

We use the parallelized LIDORT-driven AMFv6 package to derive tropospheric AMFs via online pixel-specific radiative transfer calculations, with no use of look-up tables. Our algorithm explicitly accounts for aerosol optical effects and anisotropic properties of surface reflectance, uses daily a priori aerosol and NO₂ profiles from the simulation of nested GEOS-Chem model (0.25° lat. × 0.3125° long.), and further uses Aerosol Optical Depth (AOD) data from Moderate Resolution Imaging Spectroradiometer (MODIS/Aqua) to correct GEOS-Chem simulated aerosols on a monthly basis. Figure 1 shows the procedure of using the AMFv6 package to derive the tropospheric NO₂ VCDs of POMINO-TROPOMI. Table S1 shows the retrieval parameters in POMINO-TROPOMI, in comparison with those in TM5-MP-DOMINO and POMINO v2.

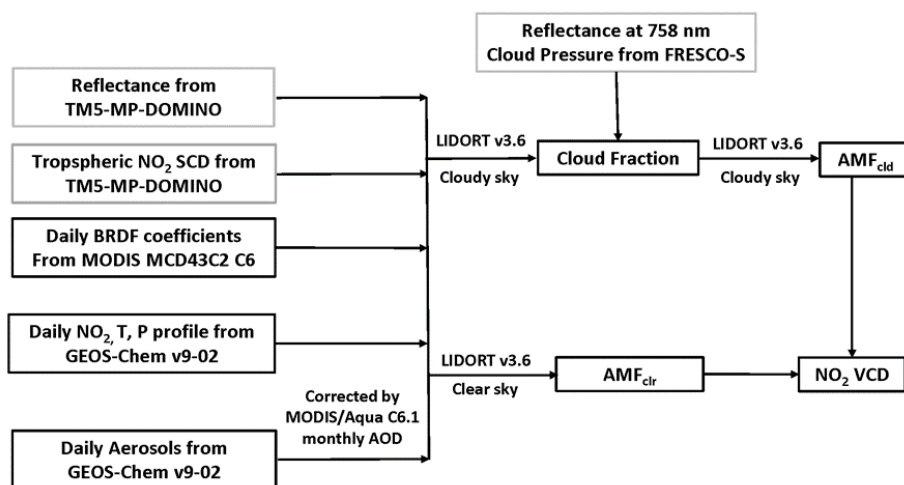


Figure 1. Flowchart of the POMINO-TROPOMI algorithm. The grey rectangles represent the parameters from the TM5-MP-DOMINO (OFFLINE) product.



The independent pixel approximation (IPA) is used to calculate AMF as a linear combination of a cloudy AMF (M_{cld}) and a clear-sky AMF (M_{clr}):

$$M = wM_{\text{cld}} + (1 - w)M_{\text{clr}} \quad (1)$$

w is the cloud radiation fraction (CRF) calculated by:

5

$$w = \frac{f_{\text{eff}}I_{\text{cld}}}{R} = \frac{f_{\text{eff}}I_{\text{cld}}}{f_{\text{eff}}I_{\text{cld}} + (1 - f_{\text{eff}})I_{\text{clr}}} \quad (2)$$

where I_{cld} denotes the radiance from the cloudy part of the pixel, I_{clr} the radiance from the clear-sky part of the pixel, f_{eff} the cloud fraction (CF), and the R the total scene radiance. Retrieval of cloud properties is a prerequisite for NO_2 retrieval. We take the effective cloud pressure (CP) from the FRESKO-S algorithm (van Geffen et al., 2019) which uses the O_2 A-band (around 758 nm) for TROPOMI trace gas retrievals. We re-calculate w and f_{eff} at the NO_2 fitting wavelength (437.5 nm). The online CF calculation is similar to (Arnaud et al., 2017) and Eskes et al., (2019), but with an explicit aerosol correction to be consistent with the following NO_2 retrieval and to remove the aerosol signal from the retrieved CF data.

15 For explicit aerosol corrections in this study, we take daily aerosol simulation results from the GEOS-Chem v9-02 nested model over East Asia, followed by a monthly AOD correction using MODIS/Aqua C6.1 AOD data. Figure 2b shows the spatial distribution of AOD in July 2018 used in clouds and NO_2 retrievals. The AOD distribution is consistent ($R = 0.42$, $N = 1447$) with that of near-surface $\text{PM}_{2.5}$ mass concentration measurements (Fig. 2a) taken from the Ministry of Ecology and Environment of China (MEE); the difference between AOD and near surface $\text{PM}_{2.5}$ is expected because they represent different parameters of aerosols.

25 The criteria to select valid pixels in this study are as follows. We exclude pixels with viewing zenith angles (VZAs) greater than 80° , with high albedos caused by ice or snow on the ground, or with quality flag (from TM5-MP-DOMINO) less than 0.5. To screen out cloudy scenes, we discard pixels with CRFs greater than 50% in the POMINO-TROPOMI product.

30 In addition to our formal POMINO-TROPOMI product (referred to as Case REF), we use two sensitivity cases to evaluate the impacts of aerosol corrections (explicit versus implicit) and the horizontal resolution of a priori NO_2 profiles (Table 2). To ensure sampling consistency, the pixels used in all cases are selected based on the CRF values in Case REF.

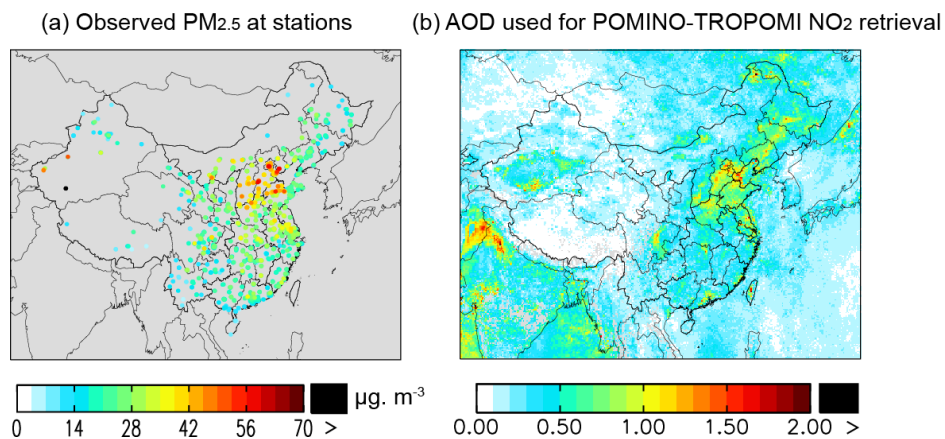


Figure 2. (a) Observed near-surface PM_{2.5} mass concentrations averaged over July 2018. Results are sampled at the times of valid TROPOMI data. (b) AOD data on a 0.05° × 0.05° grid used for the retrieval of POMINO-TROPOMI NO₂ VCDs in July 2018.

5



2.2 Ground-based MAX-DOAS measurements

We use ground-based MAX-DOAS measurements to validate the POMINO-TROPOMI NO₂ product. The MAX-DOAS measurements are from two suburban stations (Xuzhou and Nanjing) and one remote station (Fukue, Kanaya et al., 2014). Table 1 shows the geographical and time information of each MAX-DOAS site, and SI Part A describes each instrument in detail. Although Xuzhou and Nanjing are both classified as suburban sites located at university campuses, the NO₂ spatial distributions around the two sites are very different. The spatial distribution of NO₂ VCDs is relatively smooth around Xuzhou, whereas the VCDs exhibit a strong spatial gradient around Nanjing (Figure 3).

A consistent spatiotemporal sampling is crucial in comparing satellite measurements and MAX-DOAS data (Boersma et al., 2018; Lin et al., 2014; Liu et al., 2019; Wang et al., 2017). We average all valid MAX-DOAS data within ± 1 hours of the TROPOMI overpass time to obtain daily values for comparison. To reduce the influence of local events, we exclude all MAX-DOAS data whose standard deviations within the two hours exceed 20% of their mean values. We average all valid pixels within 5 km of each MAX-DOAS site to represent the respective daily satellite data. SI Part B shows how the validation results are affected by the sampling choice.

Table 1. MAX-DOAS measurement sites.

Site name	Geographical location	Measurement time
Nanjing	118.950° E, 32.118° N, 36 m	2018/07/01-2018/10/31
Xuzhou	117.142° E, 34.217° N, 92 m	2018/07/01-2018/10/31
Fukue	128.680° E, 32.750° N, 83 m	2018/07/01-2018/09/15

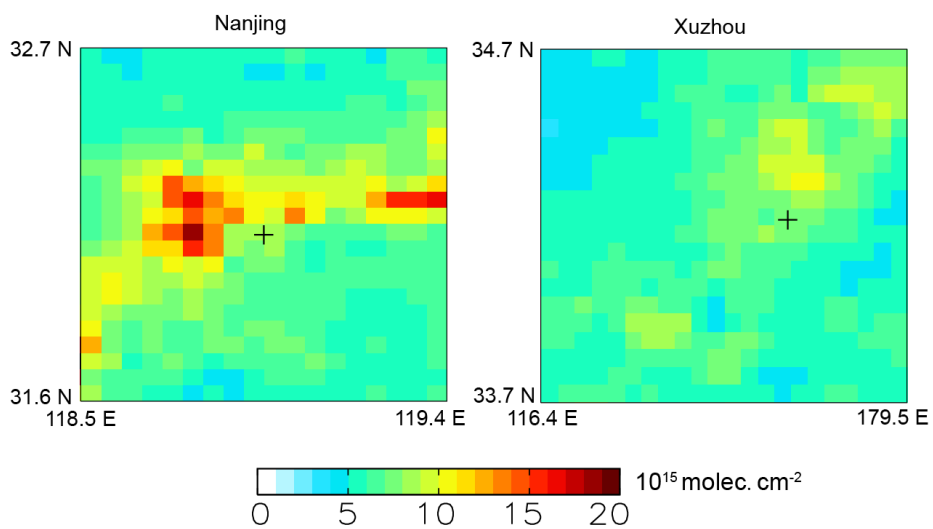


Figure 3. Spatial distributions of POMINO-TROPOMI NO_2 VCDs (on a $0.05^\circ \times 0.05^\circ$ grid) around (a) Nanjing and (b) Xuzhou MAX-DOAS measurement sites in July 2018. The MAX-DOAS sites are marked as “+”.



3. Results

3.1 POMINO-TROPOMI NO₂ VCDs over East Asia

Figure 4b shows the spatial distribution of POMINO-TROPOMI tropospheric NO₂ VCDs over East Asia on a 0.05° × 0.05° grid in July 2018. High VCD values (> 3 × 10¹⁵ molec. cm⁻²) are shown over polluted areas such as East China and India, and low values (< 1 × 10¹⁵ molec. cm⁻²) over the open ocean and the Tibetan Plateau. For comparison, the colored dots in Fig. 4a visualize the near-surface NO₂ concentrations observed at the MEE sites at the overpass time of TROPOMI. In both the VCD and the near-surface concentration maps (Fig. 4a and b), hotspots like urban centers and isolated sources can be seen clearly, due to the short lifetimes of NO_x in summer. The spatial correlation is about 0.55 (N = 1458) between the VCD and the near-surface concentration distributions.

Figure 4c shows the spatial distribution of TM5-MP-DOMINO (OFFLINE) NO₂ VCDs for comparison. The general distribution of TM5-MP-DOMINO is consistent with that of POMINO-TROPOMI with a correlation coefficient of 0.97 (N = 1091154). However, TM5-MP-DOMINO NO₂ VCD values are lower than POMINO-TROPOMI by about 35% averaged over the whole domain (Fig. 4d), by -37 – 68% over cleaner areas (POMINO-TROPOMI < 5 × 10¹⁵ molec. cm⁻²), and by 0 – 66% over more polluted areas (POMINO-TROPOMI ≥ 5 × 10¹⁵ molec. cm⁻²). TM5-MP-DOMINO does not show strong local signals at pollution hotspots like the urban center of Beijing (Fig. 5c). Over these hotspot locations, TM5-MP-DOMINO is lower than POMINO-TROPOMI by up to 5 × 10¹⁵ molec. cm⁻².

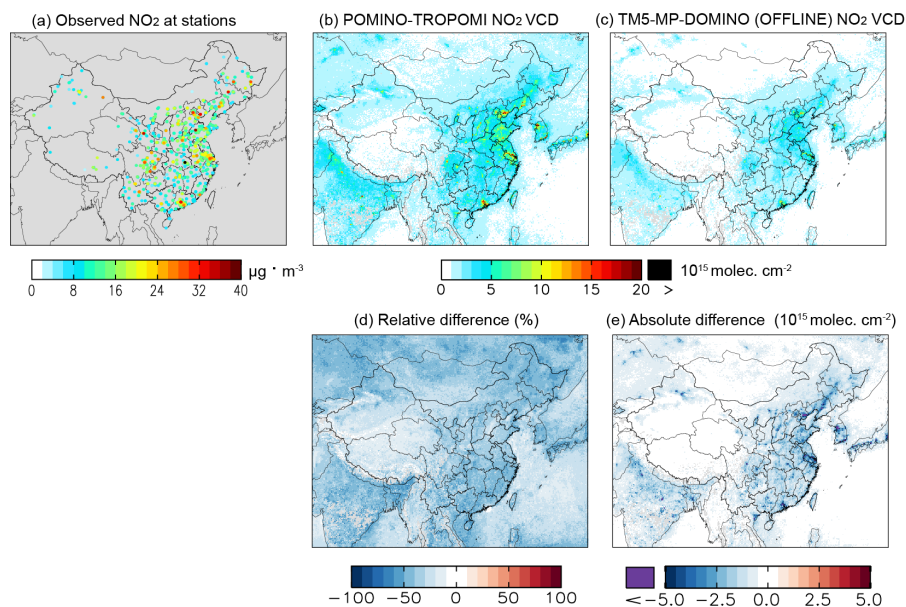


Figure 4. The spatial distribution of (a) NO₂ at monitoring stations, (b) AMFv6 derived NO₂ VCD and (c) TM5-MP-DOMINO (OFFLINE) NO₂ VCD at 0.05° × 0.05° grid in July 2018. (d) and (e) are relative and absolute difference of TM5-MP-DOMINO (OFFLINE) to POMINO-TROPOMI NO₂ VCD.

Table 2. Sensitivity experiments for the NO₂ retrieval based on the POMINO-TROPOMI algorithm.

ID	A priori NO ₂ profiles	Aerosols
Case REF (POMINO-TROPOMI)	0.25° lat. × 0.3125° long.	0.25 ° lat. × 0.3125 ° long.
Case 1	0.25° lat. × 0.3125° long.	N/A
Case 2	2° lat. × 2.5° long.	N/A

1. Case 1 – Case REF: Effects of aerosol corrections.
- 10 2. Case 2 – Case 1 : Effects of a priori NO₂ profiles (with the implicit aerosol correction).
3. Case 2 – Case REF: Joint effects of a priori NO₂ profiles and aerosol corrections.

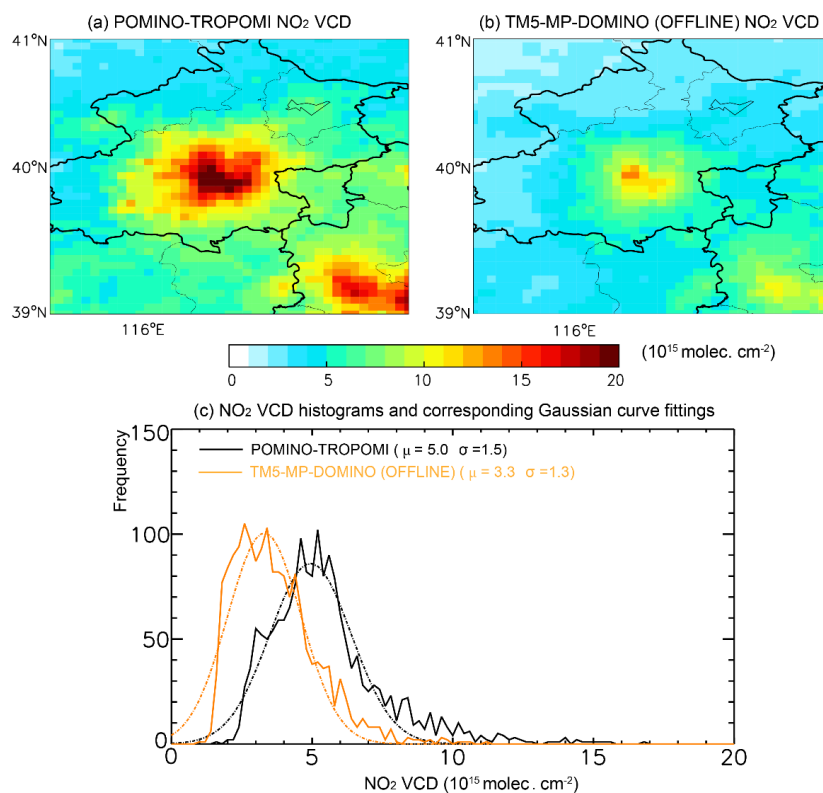


Figure 5. Spatial distributions of (a) POMINO-TROPOMI NO₂ VCDs and (b) TM5-MP-DOMINO (OFFLINE) NO₂ VCDs on a $0.05^\circ \times 0.05^\circ$ grid over Beijing and its surrounding areas averaged over July 2018. (c) Histograms of monthly NO₂ VCDs over this region. The bin size is 0.2×10^{15} molec. cm^{-2} . The black and orange dashed lines are corresponding Gaussian curve fitting of the histograms. μ is the mean value and σ is the standard deviation of a Gaussian curve fitting.



Figure 5a and b present the two products over Beijing and surrounding areas, showing a much weaker spatial gradient of NO₂ VCDs from Beijing urban center to its outskirts in TM5-MP-DOMINO than in POMINO-TROPOMI. The corresponding histograms and Gaussian fittings in Fig. 5c also show a lower mean value and a smaller standard deviation of TM5-MP-DOMINO than POMINO-TROPOMI. These results highlight the important differences between the two products at fine scales.

We further compare the two satellite products with ground-based MAX-DOAS measurements at three sites. The scatter plots in Fig. 6a and b compare the NO₂ VCDs on 63 days (from 109 pixels) over July–October 2018 with their MAX-DOAS counterparts. Different colors differentiate the sites. POMINO-TROPOMI captures the day-to-day variability in MAX-DOAS data ($R^2 = 0.75$) and shows a small normalized mean bias (NMB = 0.8%). The reduced major axis (RMA) regression shows a slope of 0.70, mainly because of the underestimate on high-NO₂ days. TM5-MP-DOMINO is also correlated with MAX-DOAS ($R^2 = 0.68$), although the correlation is weaker than our retrieval. The NMB of TM5-MP-DOMINO is much more significant (−41.9%) and the RMA regression slope is much smaller (0.42). Similar underestimates of TM5-MP-DOMINO have been discussed in their Readme document (Eskes et al., 2019) and ATBD file (van Geffen et al., 2019) in general, in Griffin et al. (2019) for Canada. Major plausible causes of the underestimate of TM5-MP-DOMINO include coarse-resolution climatological surface albedo data, coarse-resolution ($1^\circ \times 1^\circ$) a priori NO₂ profiles, implicit aerosol corrections, and uncertainties of CP from FRESCO-S.

Cloud pressures from FRESCO-S are found to be too high, i.e., the cloud top is too close to the ground, especially over China (van Geffen et al., 2019). We examine this effect by excluding the pixels with CP > 850 hPa when comparing with MAX-DOAS data. With this additional criterion, the number of valid days drop to 20. Figure 7 shows the scatter plots and corresponding RMA results. The NMB of TM5-MP-DOMINO is reduced slightly to −38.2%, and its R^2 for day-to-day variation is increased from 0.68 to 0.85. POMINO-TROPOMI still outperforms TM5-MP-DOMINO: 0.85 versus 0.85 for R^2 , 13.8% versus −38.2% for NMB, and 0.82 versus 0.56 for RMA regression slope. The improvement from excluding CP > 850 hPa scenes is larger in TM5-MP-DOMINO (with implicit aerosol corrections) than in POMINO-TROPOMI (with explicit aerosol corrections). The averaged CF of data excluding CP > 850 hPa is 0.13 (AOD = 0.63), which is much larger than the averaged value (CF = 0.06) for Fig. 6 (AOD = 0.57). This appears to imply that the overestimated CP be partly because the FRESCO-S cloud algorithm might mis-interpret heavy aerosol loadings near the ground as clouds, a common issue in satellite data (Lin and Li, 2016).

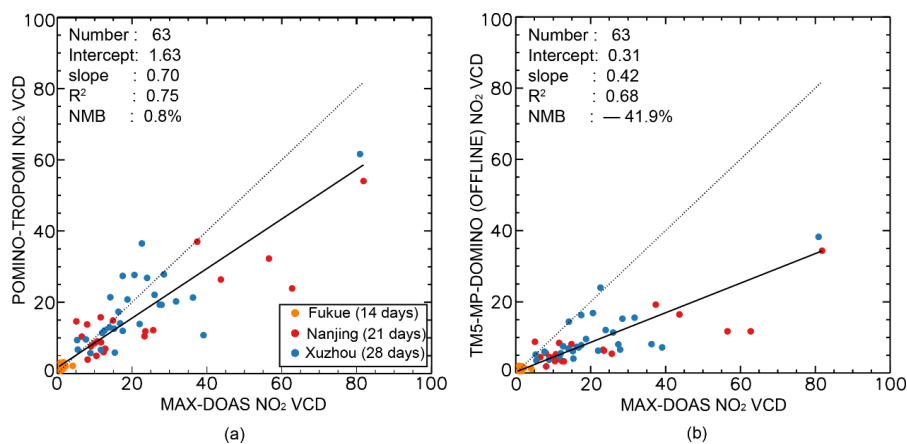


Figure 6. Scatter plot for daily NO_2 VCDs (10^{15} molec $\cdot\text{cm}^{-2}$) between MAX-DOAS and two TROPOMI NO_2 VCD products. Each colored dot represents a day and each color denotes a station. For each day, the satellite data are averaged over all pixels.

5

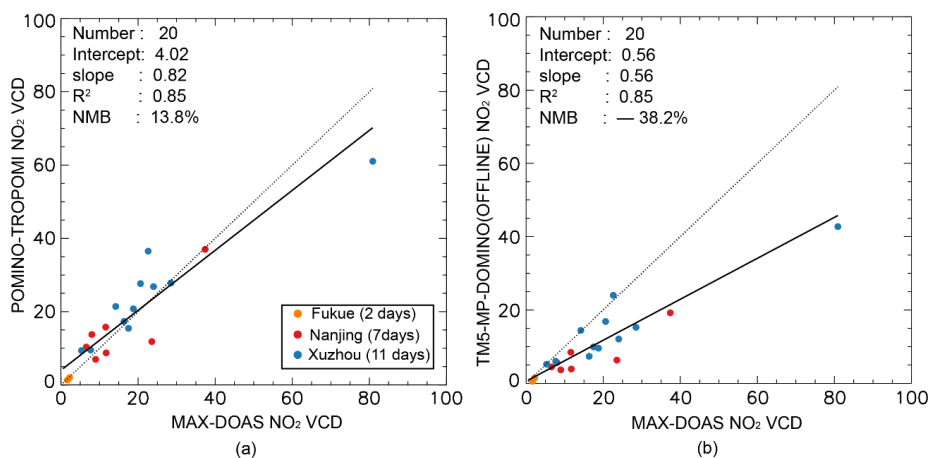


Figure 7. Scatter plot for daily NO_2 VCDs (10^{15} molec. cm^{-2}) between MAX-DOAS and two TROPOMI NO_2 VCD products with effective cloud pressures ≤ 850 hpa. Each colored dot represents a day and each color denotes a station. For each day, the satellite data are averaged over all pixels.

10



3.2 Influences of aerosol correction approaches and horizontal resolutions of a priori *NO₂ profiles*

To investigate the causes of difference between POMINO-TROPOMI and TM5-MP-DOMINO (OFFLINE), we conduct two sensitivity retrievals based on the
5 POMINO-TROPOMI algorithm (Cases 1 and 2 in Table 2). Figure 8 shows the relative (a–c) and absolute (d–f) differences between retrieval cases (REF, Case 1 and Case 2). Case 1 adopts the implicit aerosol correction for both clouds and NO₂ retrievals, as in TM5-MP-DOMINO, so the difference between REF and Case 1 indicates the effect of aerosol representation (explicit versus implicit) (Fig. 8a, d). In
10 Case 2, the high-resolution (0.25° lat. × 0.3125° long.) NO₂ profiles are replaced by low-resolution (2° lat. × 2.5° long.) profiles simulated by the GEOS-Chem global model; aerosols are represented implicitly as in Case 1. Case 2 thus mimics TM5-MP-DOMINO, which uses an implicit aerosol correction and coarse-resolution NO₂ profiles. Thus, the difference between Case 1 and Case 2 arises from the a priori
15 NO₂ profiles (Fig. 8b, e). The difference between Case 2 and REF further indicates the joint effect of using coarse-resolution a priori NO₂ profiles and an implicit aerosol correction (Fig. 8c, f).

Figure 8 shows that the individual influences of aerosol representations (explicit versus implicit) and a priori NO₂ profiles (fine versus coarse resolution) vary
20 substantially from one location to another. The impacts of aerosol corrections are most evident over the areas of heavy aerosol loadings including East China, India and parts of Southeast Asia. The implicit aerosol correction (Case 1) tends to result in lower NO₂ VCDs by 0-50% over urban areas compared to the explicit aerosol correction (Case REF) (Fig. 8a, d). By comparison, the impacts of NO₂ profiles are spatially more heterogeneous (Fig. 8b and e). Over the offshore coastal areas, using
25 coarse-resolution NO₂ profiles (Case 2) tends to overestimate the NO₂ VCDs by 30-100% relative to when high-resolution profiles are used (Case 1), due to overly (horizontal) smoothing of NO₂.

Below, we discuss these differences over two key areas including Northern East
30 China and Xinjiang. Northern Eastern China (bounded by the black rectangle in Fig. 4a) is a heavy aerosol-loaded region (Fig. 2). Over this region, an implicit rather than explicit aerosol representation results in lower NO₂ VCDs by ~25% (Fig. 8a, d), while the effect of NO₂ profiles is weaker (Fig. 8b, e). The joint effect is dominated by the effect of aerosol representation (Fig. 8c, f).

35

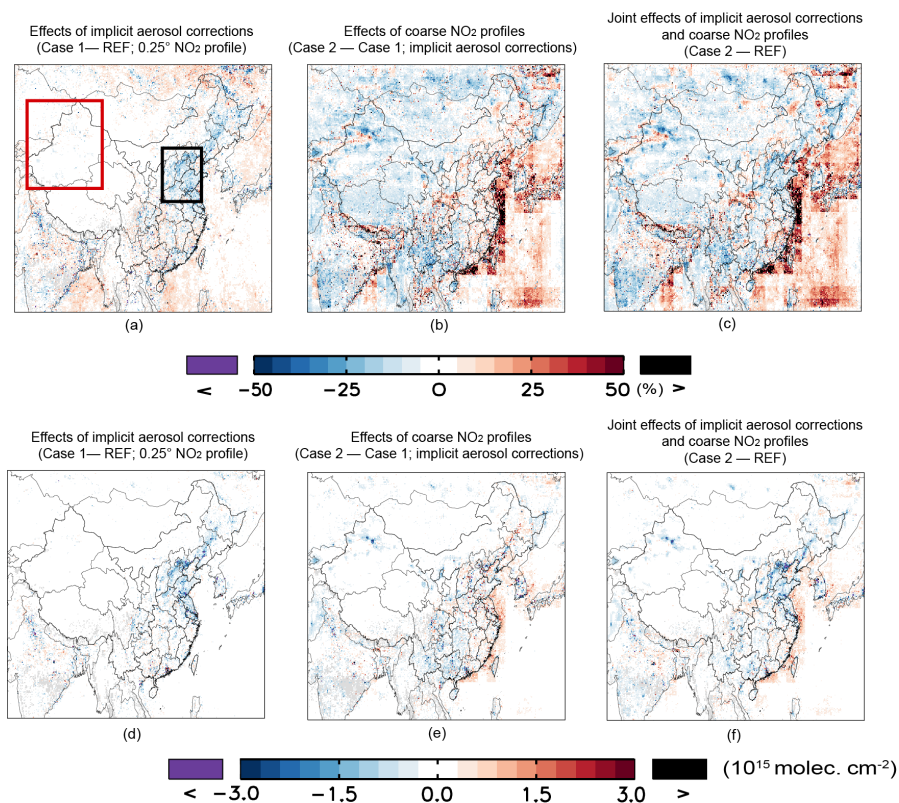


Figure 8. (a)–(c) Relative differences caused by aerosol corrections and a priori NO₂ profiles. (d)–(f) are the corresponding absolute differences. The black and red rectangles stand for Northern Eastern China and Xinjiang, respectively.

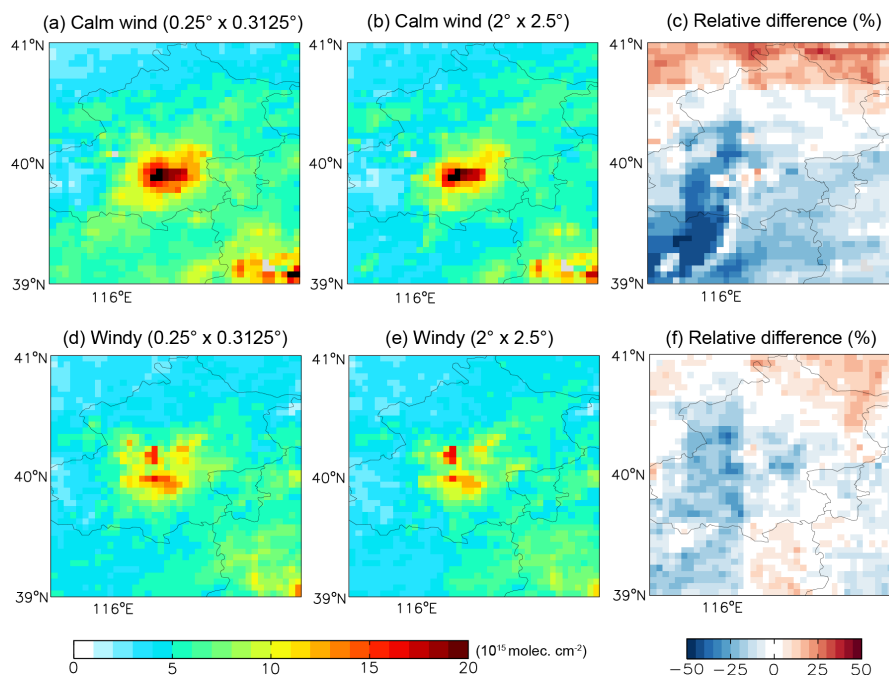


Figure 9. Spatial distributions of POMINO-TROPOMI NO_2 VCDs on a $0.05^\circ \times 0.05^\circ$ grid under calm conditions with (a) 0.25° lat. \times 0.3125° long. NO_2 profiles (Case 1), with (b) 2° lat. \times 2.5° long. profiles (Case 2), and (c) their relative differences. (d)–(f) is similar to (a)–(c) but under southward wind.

5



That the impact of a priori NO₂ profiles is relatively small over Northern Eastern China is partly because of the smearing effect by wind. Figure 9 differentiates the effects of NO₂ profiles between twenty-three windy (daily average wind speed under 500 m > 2 m s⁻¹) days and seven calm (wind speed < 2 m s⁻¹) days. The dataset of
5 wind is taken from National Aeronautics and Space Administration/Global Modeling and Assimilation Office's (NASA/GMAO's) "forward-processing" (GEOS-FP) data product with the horizontal resolution at 0.25° lat. × 0.3125° long. In the windy cases, the NO₂ VCDs are more much smoothed even at 0.3125° resolution, thus the difference of NO₂ resolutions is very small. In contrast, NO₂ VCDs exhibit much
10 stronger horizontal gradient in calm situations, which are better retrieved when high-resolution NO₂ profile are used. As calm situation is more favorable for pollutant accumulation while windy days help to dilute concentration of NO₂, so much higher NO₂ VCDs are found in Fig. 9a and b.

Xinjiang (bounded by the red rectangle in Fig. 8a) is a deserted region in West China.
15 Over Xinjiang, the resolution of a priori NO₂ profiles affects the retrieved NO₂ VCDs much more than the aerosol representation does (Fig. 8b and e). Compared to Case 1 (with high-resolution NO₂ profiles), Case 2 (with coarse-resolution profiles) leads to much lower NO₂ VCDs over the isolated urban areas which are not resolved by the coarse model.

20 4. Conclusion and Discussion

The POMINO algorithm to retrieve tropospheric NO₂ VCDs has been successfully applied to TROPOMI over East Asia. The resulting POMINO-TROPOMI product shows higher tropospheric NO₂ VCDs (by about 35% averaged over East Asia) and much clearer urban and other hotspot signals, compared to the TM5-MP-DOMINO
25 (OFFLINE) product. Further evaluation using independent MAX-DOAS measurements indicates very good performance of POMINO-TROPOMI in capturing the day-to-day variation ($R^2 = 0.75$, $N = 63$) and mean value (NMB = 0.8%) of NO₂, better than TM5-MP-DOMINO (0.68 and -41.9%, respectively).

Over heavy aerosol-loaded regions, the accuracy of retrieved NO₂ VCDs is affected
30 substantially by how aerosols are represented in the retrieval process (implicit or explicit). The implicit aerosol representation tends to underestimate the NO₂ VCDs by 0-50% over most urban areas in East Asia and by about 25% over Northern East China. Using a priori NO₂ profile data at a horizontal resolution of ~ 25 km, POMINO-TROPOMI captures the city-scale NO₂ hotspots. Reducing the horizontal
35 resolution of a priori profiles to what is typically set up by global models (100–200 km) underestimates the NO₂ hotspots and the spatial gradient surrounding them, and the effects are more pronounced in calm than in windy situations. Overall, our results provide useful information to improve TROPOMI retrieval algorithms, and offer



insight for applications to the upcoming geostationary satellite instruments including GEMS, TEMPO and Sentinel-4 Precursor.

Further work can be done to improve the retrieval algorithm for TROPOMI. The hybrid cloud retrieval method used in POMINO-TROPOMI is not optimal, because only cloud fraction but not cloud pressure is re-calculated with explicit aerosol corrections. Our previous studies for OMI shows that cloud pressure retrieval is affected by aerosols as well (Liu et al., 2019; Lin et al., 2014). Re-calculation of cloud pressure will be done in the future using the O₂-O₂ method when the O₂-O₂ SCD data are available. Second, correcting the simulated aerosol extinction vertical profiles will further improve the clouds and NO₂ retrievals (Liu et al., 2019). Third, the horizontal resolution of a priori NO₂ profiles (~ 25 km) does not match the fine footprint of TROPOMI, and further increasing the resolution will help achieve better accuracy for analyses of very fine scale pollution characteristics such as along the highways and rivers and within urban centers.

15 Acknowledgments

Acknowledgements. This study is supported by the National Natural Science Foundation of China (41775115).

Data availability. The POMINO-TROPOMI NO₂ products are available for download from: <http://www.phy.pku.edu.cn/~acm/acmProduct.php#>. The TM5-MP-DOMINO product can be download via TEMIS website: <http://www.temis.nl/airpollution/no2.html>. The near surface data of NO₂ and PM_{2.5} can be downloaded from: <http://www.cnemc.cn/sss/cskqz/>. The ground-based MAX-DOAS observations would be provided after the applications of users are approved by corresponding owners.

Author contributions. J.-T. Lin conceived the research. M.-Y. Liu and J.-T. Lin designed the experiment. M.-Y. Liu performed all calculations with some code support from H. Kong and H.-J. Weng. M.-Y. Liu and J.-T. Lin wrote the paper with inputs from K.-F. Boersma and J.-H. Eske. R. Spurr provided LIDORT. Y. Kanaya, Q. He, X. Tian, K. Qin, P.-H. Xie provided the MAX-DOAS observations. R.-J. Ni helped to process surface observations. Y.-Y. Yan and J.-X. Wang helped to analyze the relationship between meteorological and NO₂ VCD variations. All authors commented on the manuscript.

Competing interests. The authors declare no conflicts of interest.



References

- Arnoud, A., Mattia, P., Maarten, S., Veefkind, J. P., Loyola, D., and Wang, P.: Sentinel-5 precursor/TROPOMI Level 2 Product User Manual KNMI level 2 support products, Royal Netherlands Meteorological Institute (KNMI), De Bilt, the Netherlands, ATBD, 2017.
- 5 Boersma, K. F., Eskes, H. J., and Brinksma, E. J.: Error analysis for tropospheric NO₂ retrieval from space, *Journal of Geophysical Research: Atmospheres*, 109, doi: 10.1029/2003JD003962, 2004.
- Boersma, K. F., Eskes, H. J., Dirksen, R. J., van der A, R. J., Veefkind, J. P., Stammes, P., Huijnen, V., Kleipool, Q. L., Sneep, M., Claas, J., Leitão, J., Richter, A., Zhou, Y., and Brunner, D.: An improved tropospheric NO₂ column retrieval algorithm for the Ozone Monitoring Instrument, *Atmos. Meas. Tech.*, 4, 1905-1928, doi: 10.5194/amt-4-1905-2011, 2011.
- 10 Boersma, K. F., Eskes, H. J., Richter, A., De Smedt, I., Lorente, A., Beirle, S., van Geffen, J. H. G. M., Zara, M., Peters, E., Van Roozendaal, M., Wagner, T., Maasakkers, J. D., van der A, R. J., Nightingale, J., De Rudder, A., Irie, H., Pinardi, G., Lambert, J. C., and Compernelle, S. C.: Improving algorithms and uncertainty estimates for satellite NO₂ retrievals: results from the quality assurance for the essential climate variables (QA4ECV) project, *Atmos. Meas. Tech.*, 11, 6651-6678, doi: 10.5194/amt-11-6651-2018, 2018.
- 15 Dentener, F., van Weele, M., Krol, M., Houweling, S., and van Velthoven, P.: Trends and inter-annual variability of methane emissions derived from 1979-1993 global CTM simulations, *Atmos. Chem. Phys.*, 3, 73-88, doi: 10.5194/acp-3-73-2003, 2003.
- 20 Eskes, H., van Geffen, J. H. G. M., Boersma, F., Sneep, M., ter Linden, M., and Veefkind, P.: Sentinel-5P TROPOMI high-resolution nitrogen dioxide observations, American Geophysical Union Fall Meeting, Walter E Washington Convention Center, Washington, D.C., 2018, 2018.
- Eskes, H. J., Eichmann, K. U., Lambert, J. C., Loyola, D., Veefkind, J. P., Dehn, A., and Zehner, C.: S5P Mission Performance Centre Nitrogen Dioxide [L2_NO2__] Readme, Royal Netherlands Meteorological Institute (KNMI) De Bilt, the Netherlands 01.03.00, 2019.
- 25 Goryl, P., Zehner, C., and Laur, H.: Sentinel-5 Precursor Calibration and Validation Plan for the Operational Phase, Royal Netherlands Meteorological Institute (KNMI), De Bilt, the Netherlands, 2017.
- 30 Griffin, D., Zhao, X., McLinden, C. A., Boersma, F., Bourassa, A., Dammers, E., Degenstein, D., Eskes, H., Fehr, L., Fioletov, V., Hayden, K., Kharol, S. K., Li, S.-M., Makar, P., Martin, R. V., Mihele, C., Mittermeier, R. L., Krotkov, N., Sneep, M., Lamsal, L. N., Linden, M. t., Geffen, J. v., Veefkind, P., and Wolde, M.: High-Resolution Mapping of Nitrogen Dioxide With TROPOMI:



- First Results and Validation Over the Canadian Oil Sands, *Geophysical Research Letters*, 46, 1049-1060, doi: 10.1029/2018gl081095, 2019.
- Hoek, G., Krishnan, R. M., Beelen, R., Peters, A., Ostro, B., Brunekreef, B., and Kaufman, J. D.: Long-term air pollution exposure and cardio- respiratory mortality: a review, *Environmental Health*, 12, 43, doi: 10.1186/1476-069x-12-43, 2013.
- Kanaya, Y., Irie, H., Takashima, H., Iwabuchi, H., Akimoto, H., Sudo, K., Gu, M., Chong, J., Kim, Y. J., Lee, H., Li, A., Si, F., Xu, J., Xie, P. H., Liu, W. Q., Dzhola, A., Postlyakov, O., Ivanov, V., Grechko, E., Terpugova, S., and Panchenko, M.: Long-term MAX-DOAS network observations of NO₂ in Russia and Asia (MADRAS) during the period 2007-2012: instrumentation, elucidation of climatology, and comparisons with OMI satellite observations and global model simulations, *Atmos. Chem. Phys.*, 14, 7909-7927, doi: 10.5194/acp-14-7909-2014, 2014.
- Krotkov, N. A., McLinden, C. A., Li, C., Lamsal, L. N., Celarier, E. A., Marchenko, S. V., Swartz, W. H., Bucsela, E. J., Joiner, J., Duncan, B. N., Boersma, K. F., Veefkind, J. P., Levelt, P. F., Fioletov, V. E., Dickerson, R. R., He, H., Lu, Z., and Streets, D. G.: Aura OMI observations of regional SO₂ and NO₂ pollution changes from 2005 to 2015, *Atmos. Chem. Phys.*, 16, 4605-4629, doi: 10.5194/acp-16-4605-2016, 2016.
- Laughner, J. L., Zare, A., and Cohen, R. C.: Effects of daily meteorology on the interpretation of space-based remote sensing of NO₂, *Atmos. Chem. Phys.*, 16, 15247-15264, doi: 10.5194/acp-16-15247-2016, 2016.
- Lin, J., and Li, J.: Spatio-temporal variability of aerosols over East China inferred by merged visibility-GEOS-Chem aerosol optical depth, *Atmospheric Environment*, 132, 111-122, doi: <https://doi.org/10.1016/j.atmosenv.2016.02.037>, 2016.
- Lin, J. T., McElroy, M. B., and Boersma, K. F.: Constraint of anthropogenic NO_x emissions in China from different sectors: a new methodology using multiple satellite retrievals, *Atmos. Chem. Phys.*, 10, 63-78, doi: 10.5194/acp-10-63-2010, 2010.
- Lin, J. T., Martin, R. V., Boersma, K. F., Sneep, M., Stammes, P., Spurr, R., Wang, P., Van Roozendael, M., Clémer, K., and Irie, H.: Retrieving tropospheric nitrogen dioxide from the Ozone Monitoring Instrument: effects of aerosols, surface reflectance anisotropy, and vertical profile of nitrogen dioxide, *Atmos. Chem. Phys.*, 14, 1441-1461, doi: 10.5194/acp-14-1441-2014, 2014.
- Lin, J. T., Liu, M. Y., Xin, J. Y., Boersma, K. F., Spurr, R., Martin, R., and Zhang, Q.: Influence of aerosols and surface reflectance on satellite NO₂ retrieval: seasonal and spatial characteristics and implications for NO_x emission constraints, *Atmos. Chem. Phys.*, 15, 11217-11241, doi: 10.5194/acp-15-11217-2015, 2015.



- Liu, M., Lin, J., Boersma, K. F., Pinardi, G., Wang, Y., Chimot, J., Wagner, T., Xie, P., Eskes, H., Van Roozendaal, M., Hendrick, F., Wang, P., Wang, T., Yan, Y., Chen, L., and Ni, R.: Improved aerosol correction for OMI tropospheric NO₂ retrieval over East Asia: constraint from CALIOP aerosol vertical profile, *Atmos. Meas. Tech.*, 12, 1-21, doi: 10.5194/amt-12-1-2019, 2019.
- 5 Lorente, A., Folkert Boersma, K., Yu, H., Dörner, S., Hilboll, A., Richter, A., Liu, M., Lamsal, L. N., Barkley, M., De Smedt, I., Van Roozendaal, M., Wang, Y., Wagner, T., Beirle, S., Lin, J. T., Krotkov, N., Stammes, P., Wang, P., Eskes, H. J., and Krol, M.: Structural uncertainty in air mass factor calculation for NO₂ and HCHO satellite retrievals, *Atmos. Meas. Tech.*, 10, 759-782, doi: 10.5194/amt-10-759-2017, 2017.
- 10 McLinden, C. A., Fioletov, V., Boersma, K. F., Kharol, S. K., Krotkov, N., Lamsal, L., Makar, P. A., Martin, R. V., Veeffkind, J. P., and Yang, K.: Improved satellite retrievals of NO₂ and SO₂ over the Canadian oil sands and comparisons with surface measurements, *Atmos. Chem. Phys.*, 14, 3637-3656, doi: 10.5194/acp-14-3637-2014, 2014.
- Ott, L. E., Pickering, K. E., Stenchikov, G. L., Allen, D. J., DeCaria, A. J., Ridley, B., Lin, R.-F.,
15 Lang, S., and Tao, W.-K.: Production of lightning NO_x and its vertical distribution calculated from three-dimensional cloud-scale chemical transport model simulations, *Journal of Geophysical Research: Atmospheres*, 115, doi: doi:10.1029/2009JD011880, 2010.
- Russell, A. R., Perring, A. E., Valin, L. C., Bucsele, E. J., Browne, E. C., Wooldridge, P. J., and
20 Cohen, R. C.: A high spatial resolution retrieval of NO₂ column densities from OMI: method and evaluation, *Atmos. Chem. Phys.*, 11, 8543-8554, doi: 10.5194/acp-11-8543-2011, 2011.
- Shindell, D. T., Faluvegi, G., Koch, D. M., Schmidt, G. A., Unger, N., and Bauer, S. E.: Improved Attribution of Climate Forcing to Emissions, *Science*, 326, 716-718, doi: 10.1126/science.1174760, 2009.
- van Geffen, J. H. G. M., Eskes, H. J., Boersma, K. F., Maasackers, J. D., and Veeffkind, J. P.:
25 TROPOMI ATBD of the total and tropospheric NO₂ data products (issue 1.4.0), Royal Netherlands Meteorological Institute (KNMI), De Bilt, the Netherlands, 2019.
- Veeffkind, J. P., Aben, I., McMullan, K., Förster, H., de Vries, J., Otter, G., Claas, J., Eskes, H. J., de Haan, J. F., Kleipool, Q., van Weele, M., Hasekamp, O., Hoogeveen, R., Landgraf, J., Snel, R., Tol, P., Ingmann, P., Voors, R., Kruizinga, B., Vink, R., Visser, H., and Levelt, P. F.: TROPOMI
30 on the ESA Sentinel-5 Precursor: A GMES mission for global observations of the atmospheric composition for climate, air quality and ozone layer applications, *Remote Sensing of Environment*, 120, 70-83, doi: <https://doi.org/10.1016/j.rse.2011.09.027>, 2012.



Wang, Y., Lampel, J., Xie, P., Beirle, S., Li, A., Wu, D., and Wagner, T.: Ground-based MAX-DOAS observations of tropospheric aerosols, NO₂, SO₂ and HCHO in Wuxi, China, from 2011 to 2014, *Atmos. Chem. Phys.*, 17, 2189-2215, doi: 10.5194/acp-17-2189-2017, 2017.

Williams, J. E., Boersma, K. F., Le Sager, P., and Verstraeten, W. W.: The high-resolution version of TM5-MP for optimized satellite retrievals: description and validation, *Geosci. Model Dev.*, 10, 721-750, doi: 10.5194/gmd-10-721-2017, 2017.

Zara, M., Boersma, K. F., De Smedt, I., Richter, A., Peters, E., van Geffen, J. H. G. M., Beirle, S., Wagner, T., Van Roozendael, M., Marchenko, S., Lamsal, L. N., and Eskes, H. J.: Improved slant column density retrieval of nitrogen dioxide and formaldehyde for OMI and GOME-2A from QA4ECV: intercomparison, uncertainty characterisation, and trends, *Atmos. Meas. Tech.*, 11, 4033-4058, doi: 10.5194/amt-11-4033-2018, 2018.

Zhou, Y., D. Brunner, R. J. D. Spurr, K. F. Boersma, M. Sneep, C. Popp, and B. Buchmann (2010), Accounting for surface reflectance anisotropy in satellite retrievals of tropospheric NO₂, *Atmos. Meas. Tech.*, 3(5), 1185-1203.